JOURNAL OF INTERNATIONAL MARITIME SAFETY, ENVIRONMENTAL AFFAIRS, AND SHIPPING
2020, VOL. 4, NO. 4, 135–150
https://doi.org/10.1080/25725084.2020.1840859

Taylor & Francis
Taylor & Francis Group

Safety comparison analysis between LNG/LH_2 for bunkering operation

Charalampos Tofalos, Byongug Jeong and Hayoung Jang

Department of Naval Architecture, Ocean and Marine Engineering, University of Strathclyde, Glasgow, UK

ABSTRACT

This paper was to conduct a comparative analysis between two credible marine fuels: LNG and hydrogen from safety perspective. As the first step, a bulk carrier 80,000 DWT Kamsarmax was selected as the case ship, whereas the conceptual design of retrofitting the bunkering system was implemented. In order to gain important insights into risk levels of those fuels associated with bunkering, accidental fire/explosion scenarios were developed, and the potential risks of those adverse situations were quantified. The results were interpreted as a form of the levels of safety zones applicable for bunkering. As the first attempt to compare the risk of two promising marine fuels, this paper is highly believed to give some meaningful insights into proper understanding of risk levels, thereby establishing safety practices and conducting future regulatory frameworks to mitigate those risks accordingly.

ARTICLE HISTORY
Received 5 October 2020
Accepted 19 October 2020

KEYWORDS
Safety assessment; LNG; LH_2; hydrogen; natural gas; bunkering process

Introduction

As awareness of environmental pollution and environmental issues has been raised around the world, and 2.5% of global gaseous pollutants are generated from ships, the shipping industry has enacted environmental regulations to reduce global pollution through the IMO. The use of alternative fuels such as LNG and LH_2 is becoming an increasingly attractive solution and its demand is growing rapidly.

The use of these two fuels will undoubtedly contribute to reducing air emissions caused by the shipping sector. However, the main issue of common safety concerns is still raised. Since accidental release of flammable substances can lead to fire and explosion, the use of these fuels on existing ships requires the installation and use of new components that are susceptible to fatigue. However, since these fuels have only begun to be used in the transport sector very recently, the legislative system has limitations and drawbacks in the field of safety and does not provide a clear quantitative term. Therefore, several rules, regulations, guidelines and standards have been established to ensure safety.

The IMO has developed the International Safety Code for vessels that use low-ignition fuels (IGF code) which covers all provisions to adjust and install machinery, compartments, systems and equipment of ship (Code 2014). To minimize the potential risk posed by the use of such high-energy fuel mass, other international organizations and governments have established guidelines and regulations on the safety of ships using LNG.

Thereby, strict environmental regulations may increase the demand for ships using alternative fuels such as LNG and LH_2, which are likely to increase the number of accidents related to the leakage of both fuels. Hence, in order to strengthen existing regulations and ensure the development as well as improvement of safer supply technologies, there has been a need to evaluate and identify the risks associated with the two fuel supply processes and to compare results.

The bunkering operation is inevitable for ships which use LNG or LH_2 as fuel. The most common bunkering method for both fuels is to transfer the liquid fuel from the terminal to the receiving ship. The process of bunkering the two fuels requires great care because the cryogenic transport of the two liquids entails many risks. In addition, the worrying part of the bunkering process is large-scale refuelling operations for seafaring ships, given the devastating effects of a massive accidental release of fuel. Due to the lack of LNG and LH_2 fuel refuelling infrastructure worldwide, much of the bunkering is done by ship.In line with this, it is imperative that all refuelling procedures are carried out with great care to avoid any leakage of liquid fuel or vapour, and to check all possible sources of ignition. This is because in case of leakage on the deck and formation of vapour clouds, there is a certain concentration that will reach the source of ignition and will cause a fire.

Past research

One of the major tasks of the IMO Committee in 2016 was the approval of the IGF Code, which represents the International Safety Code for ships using gas or other

CONTACT Byongug Jeong byongug.jeong@strath.ac.uk Department of Naval Architecture, Ocean and Marine Engineering, University of Strathclyde, Glasgow G4 0LZ

fuels such as ethane and methanol. The main purpose of this Code is to establish a framework that regulates the construction, installation, monitoring and control of machinery and machinery of ships fueled with low-ignition fuels to ensure the safety of crew and cargo and significantly reduce accidents.. This regulation necessarily applies to vessels with a total capacity of 500 tons or more and using low-ignition gas fuel.

However, although several organizations and governments have conducted studies to develop and establish a regulatory framework related to bunkering, there are many limitations (ABS 2014). Currently, LNG and LH_2 related regulations do not have direct regulations related to bunkering, and their applicable scope is very limited (DNV 2014).

Literature review

In the past, LNG carriers mainly produced steam to propel steam turbines, but advances in engine technology today make it possible to use dual fuel engines (Schlick 2014).

Accordingly, the number of LNG-fueled vessels has continued to grow rapidly, and various safety studies on LNG have been continued. Qiao and Zhang (2010) concluded that LNG used as fuel in ships is in a special circumstance where it is stored in a liquid state of −142 °C to −162 °C with LNG is the high operating pressure of 300 bar of the power supply system (FGSS), so the main variables that affect the explosion are leakage rate, ventilation conditions, wind speed and the gas density. A comparative study on the safety of land and marine terminals was conducted by Aneziris et al. (2014). In terms of the bunkering process, ship-to-ship requires special attention as it can be the most dangerous method due to the wide range of movement between the two ships (Jeong et al. 2017).

In the meantime, hydrogen (H_2) is one of the cleanest fuels, as mentioned above. The application of firm environmental regulations has led to a significant rise in its demand, which is expected to continue to increase rapidly in the future. The main hazards associated with the use of hydrogen are the causes of fire due to the high flammability of hydrogen, known as the possibility of explosion at concentrations of 18.3% −59% (Farese and Ivanova 2013). It can also cause cracking and failure of metals such as high-strength steel, aluminum alloys and titanium due to its ability to embrittle metals (Ruiz et al. 2015). Another study using a natural gas reforming process in a hydrogen production unit found that jet fires had the highest mortality rates and affected the largest area of 5102 m^2 (Jafari, Zarei, and Badri 2012).

Liquid hydrogen (LH_2) also investigated as a marine fuel by describing its physical and combustion properties. LH_2 was compared to LNG because maritime regulations formalized and addressed the use of LNG. This comparison reveals that there are no specific regulations for the use of hydrogen as marine fuel (Klebanoff, Pratt, and LaFleur 2017).

Research gap

Despite the growing interest in the shipping industry for new green fuels such as LNG and LH_2, current regulations and rules are insufficient in terms of safety. There are also safety vulnerabilities in the two IGF and IGC regulations governing the configuration, design and operating systems of these vessels. While several agencies have attempted to cover safety gaps while bunkering these fuels, they have provided only a general analysis rather than a comparative proposal to create exclusion zones and other safety valves.

Another fact observed in the investigation of the existing literature is that the same rules apply because there is no clear separation of the two fuels, and systems such as the bunkering system and fuel supply system (FGSS) of LNG and LH_2 fueled ships have the highest level of risk. Nevertheless, it has never been systematically studied.

It can be concluded that systematic and thorough risk assessment studies are desperately needed to strengthen the safety regulations of these vessels. Therefore, the aim of this paper is to contribute to the improvement of the safety of LNG fuelled and LH_2 fuelled vessels by investigating the safety of LNG and LH_2-fuelled vessels during a process involving the highest risk levels – bunkering.

Method applied

Along with the bunkering method of two fuels, we mainly perform a theoretical approach to frequency and result analysis to investigate the safety hazards of both fuels during the bunkering process. Research and comparison of the safety factor derived from bunkering of two fuels (LNG and LH_2) through the large amount of research conducted in previous studies as shown in Figure 1.

Case vessel and bunkering system description

The selected research vessels are all standard models of DNV GL, IGF and are assumed to have been converted to LNG fueled propulsion vessels. This ship is an 80,000 DWT Kamsarmax bulk carrier that conducts international voyages from North America to Northwest Europe. The specifications of the ship are shown in Table 1. In this study, both fuels are studied in the same state (liquid form) in a bunkering system, so the construction requirements of both fuels are assumed to be the same.

Based on the operational profile of the ship, which is at 85% of MCR, the operational speed in the design

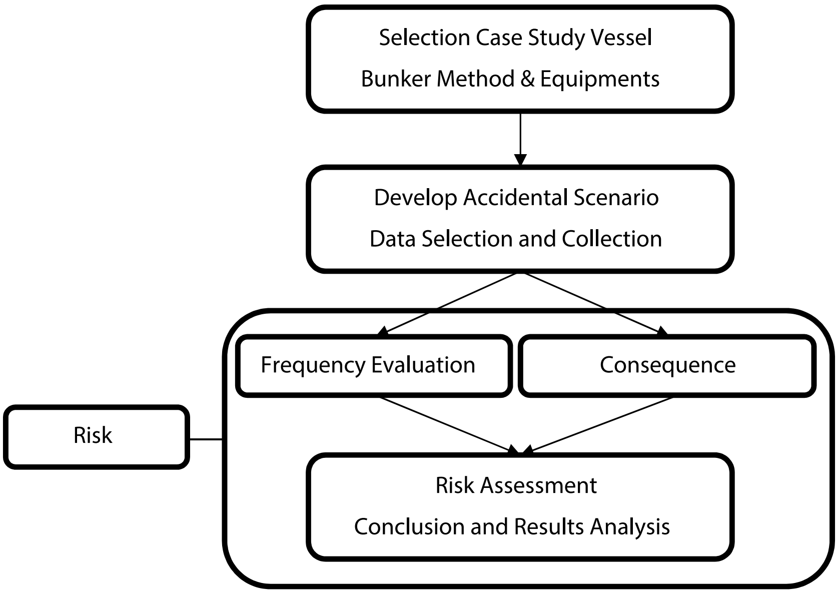

Figure 1. Project flowchart.

Table 1. Specifications of case study vessel.

Main Engine (Dual Fuel)	MAN B&W 6S60ME-C8.5-GI
Length O.A (L.O.A)	229.0 m
Breadth (B)	32.26 m
Depth (D)	20.01 m
Deadweight (DWT)	80,000 t
MCR	14,680 kW
NCR	12,138 kW
Liquid Gas Fuel Tank	2,600 m3 (IMO C type)

draught is 14.3 NM/h equal to 343.2 NM/day. The ship is estimated to consume around 23.27 t/day when SGC of NCR is 135.2 g/kWh. The ship, according to its operational profile from North America to North Europe and back, is designed to have a capacity of 500–600 m^3, provided that the ship consumes LNG only in emission control areas. Based on its design and operational profile, a tank with a capacity of 2200 to 2600 m^3 (in the case of IMO C) is approximately required for a full trip from the USA to Europe. This requires a month for a full voyage to cover the longest distance the vessel is built, so the bunkering frequency is 12 times a year. The installation of liquid gas fuel piping follows the construction requirements of IGF code. The two bunkering stations on the ship are located on the port and starboard side of the accommodation in order to be close to the installed tank and to avoid the expansion of the pipelines and the involvement in the area of unloading and loading of the ship.

Due to the small space on the deck of the bulk carrier, the LNG tank is installed in a superstructure at the rear of the accommodation block. Figure 2 depicts the piping diagram of the LNG bunkering system that was designed.

The bunkering system fundamentally consists of three lines, the main bunker line, the vapour line and the inert gas line. In this particular case study ship, as the tank is IMO C, it can hold the vapour produced during the bunkering process. Thereby, the vapour does not return to the feeder side and it is not designed in the system. Furthermore, the inert gas line is assumed to be provided onboard. In the main bunkering line, emergency shutdown valves (ESD) have been installed in compliance with the load transfer regulations.

The pipes of the bunkering system are designed with a diameter of 0.15 m and their length is calculated at 45 m total, taking into account the breadth of the

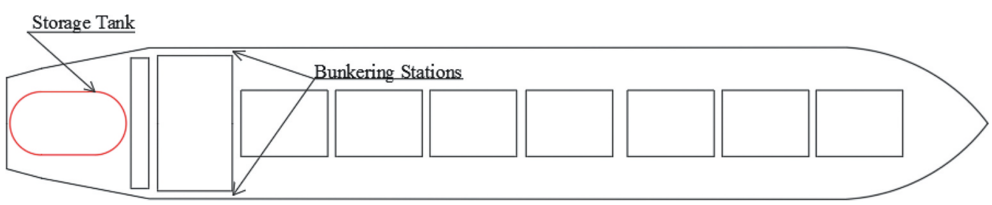

Figure 2. Conceptual arrangement of LNG bunkering system.

ship, 32.26 m and the distance that the pipes have to cover to the tank. Since the bunkering operation is not ship-to-ship (STS), it is assumed that the velocity of the fluid is 5 m/s, so the bunker tank (2,600 m^3) needs around 8 h to fill during a bunkering, requiring this way 96 h/year. The installation of the pipes as well as the components of the bunkering piping system on the case study vessel can support pipeline to ship (PTS) and truck to ship (TTS).

Table 2 lists the equipment of the conceptual bunkering piping system that were illustrated in Figure 3. In Figure 3, the line and the components of liquefied gas are illustrated in red, whereas the line and the components of N_2 are illustrated in blue. Table 2 does not calculate the inert line because it is not directly involved in the bunkering process.

Accidental scenario and data collection

Without examining the human factor, an analysis of the risks and accidental scenario that may arise during bunkering operation of the two fuels is conducted taking into account the equipment and components of the bunkering system and their leakage probability.

The fuel leak accident is the main risk that can occur during the bunkering operation. The risks that may arise from the bunkering process will be identified before the quantitative risk assessment. The first step is to define the equipment that makes up the system to be tested, as well as its clear dimensions and the number of equipment necessary. The second step is to identify the phase at which fuel is found at the point of leakage, which will determine the effects it may cause. Furthermore, the method with which the procedure is performed to play an important role in the whole process of identifying risks in the bunkering process. The bunkering method chosen for this particular case study vessel is not STS, but TTS or PTS, both of which are common methods to LNG and LH_2 (see Figure 4).

It should be noted that only the main line of the bunkering is exposed to the risk of leakage, since the steam line due to the use of IMO C tanks on certain case study vessels is not required and the N_2 line is not actively involved. Thus, in the scenario where the current project is focused, the main line and the components are investigated.

In terms of monitoring systems, since the bunkering process takes place outdoors, there is no need to install gas detection devices in accordance with regulations. Therefore, possible leakage can only be detected by a monitor. Another important factor in the case study scenario is that ventilation occurs naturally during the

Table 2. Bunker system equipment.

Equipment	Size (mm)	Bunker Line
LNG Tank	150	1
Pressure Relief Valve	150	3
Pressure Indicators	50	2
Main Line Pipes	150	45
ESD Valve	150	4
Manual Valve	100	2
Main Line Flanges	150	12

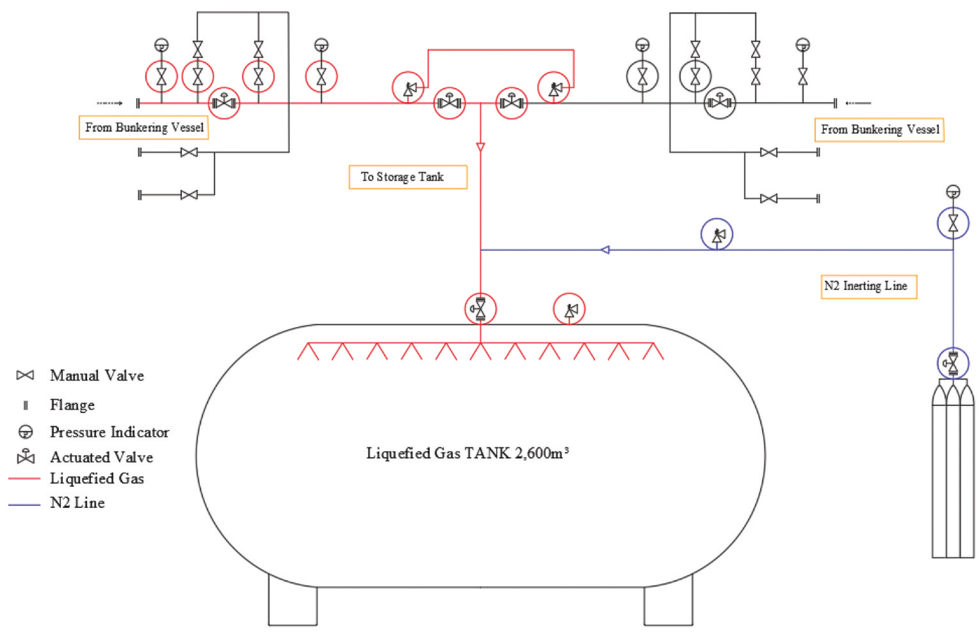

Figure 3. Conceptual design of bunkering piping system.

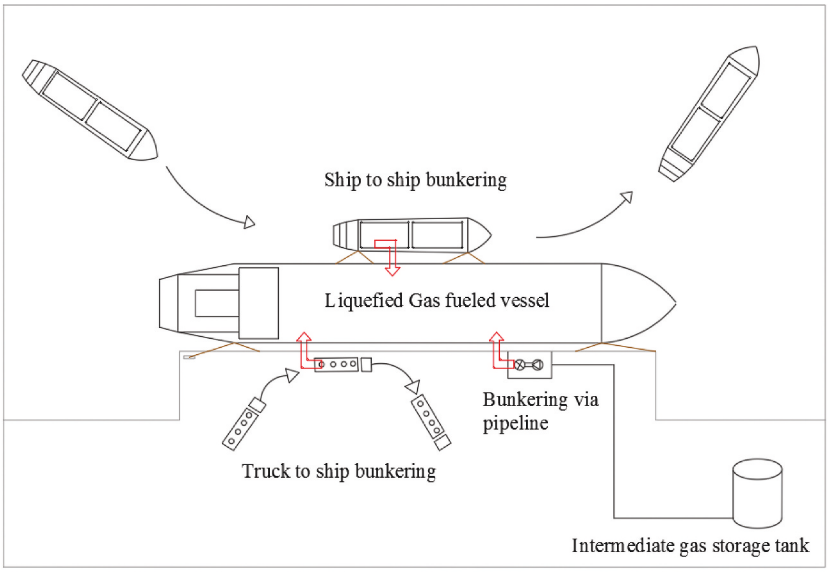

Figure 4. Bunkering methods.

bunkering process. The pressure of the liquid fuel is considered to be 3 bar, the transport temperature for LNG is −162 ° C and −253 ° C for LH_2.

In order to develop accurate and reliable results, the case vessel is one of the DNV GL-certified structures in cooperation with a transportation company and hydrocarbon release database (HCRD) data was selected to accurately estimate the leakage frequency of the components that make up the piping system (DNV 2012a). This database is limited to the UK oil and gas industry but is comprehensive with a record of leaks of over 20 years.

Risk analysis

Safety assessment is conducted through a quantitative risk assessment process using frequency and consequence analysis. As a directly related risk analysis method, frequency and consequence analysis investigates and analyzes fire and explosion hazards, which are the possible consequences of LNG and LH_2 fuel leakage accidents during bunkering operations.

The dimensions of the components of the bunkering system range from 12.5 mm to 25 mm. The frequency of accidents during the bunkering process takes place in an open space shown in the following equations:

$$F_{PoolFire} = F_{InitialLeak} * P_{Imm.Ignition} \qquad \text{Eq.(1)}$$

$$_{FlashFire} = F_{InitialLeak} * P_{LateIsol.Leak} * P_{Suc.Ven} * P_{Del.Ignition} * P_{NotCong.} \qquad \text{Eq.(2)}$$

$$F_{Explosion} = F_{InitialLeak} * P_{LateIsol.Leak} * P_{Suc.Ven} * P_{Del.Ignition} * P_{Congested} \qquad \text{Eq.(3)}$$

Where,

P = Probability

F = Frequency per year

Consequence analysis is a process that represents consequences in the event of hazards such as explosions, fires, leaks and evaporation, and is directly related to the size of the leak. It can be performed using recognized models that have the ability to identify and determine the effects of hazards on humans, structure and equipment. Figure 5 shows the general consequence analysis process models.

As shown in Figure 6, risk fundamentally determines the outcome of an accident. The effect and consequences of a risk are estimated in terms of loss of human life, injuries and financial consequences in the event that the outcome of the risk is catastrophic.

The study focuses on the likelihood of explosion and fire hazards from fuel leaks during the LNG and LH_2 bunkering process not taking into account the immediate danger to human lives.

Case study

According to the sequence of Figure 1, frequency and results analysis were performed based on the selected bunkering system and case ship.

Frequency evaluation

Initial leak frequency

The bunkering process takes place outdoors and the pipes and fittings are not double walled, so there is a high probability of leakage. Since the initial leakage frequency of bunkering system components is expected to range from 50 mm to 150 mm, it is analyzed in the table below. Therefore, all scenarios are

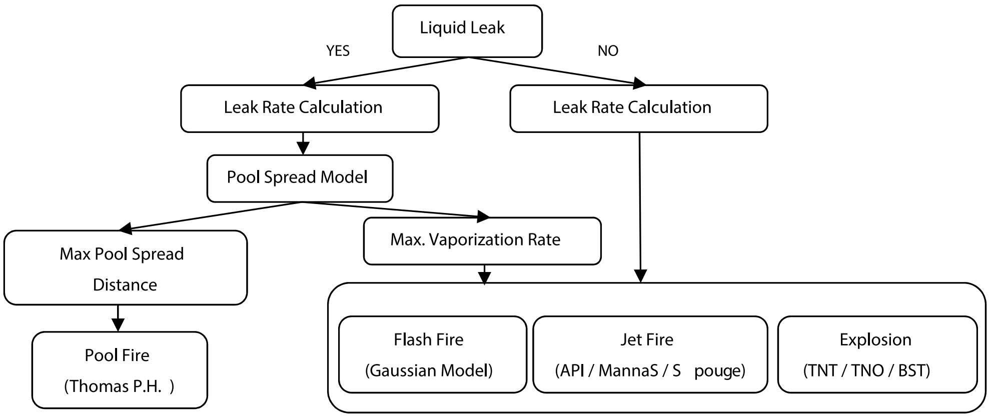

Figure 5. General approach of consequence analysis models.

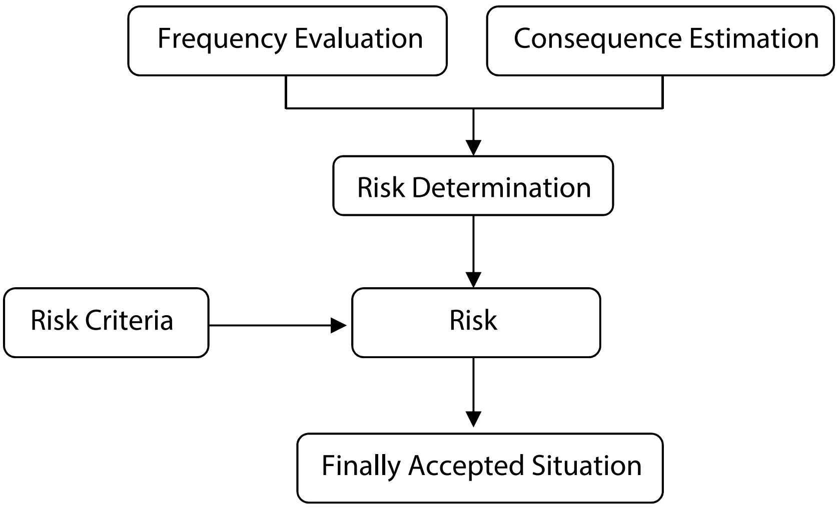

Figure 6. Layout of risk assessment.

analyzed in four groups: 1–3 mm, 10–50 mm, 50–150 mm and full bore rupture> 150 mm according to the data of DNV leak frequency.

Figure 7 depicts the results of the total calculations that derived from Table 3. The results show a moderate leak frequency which is affected by the frequency of

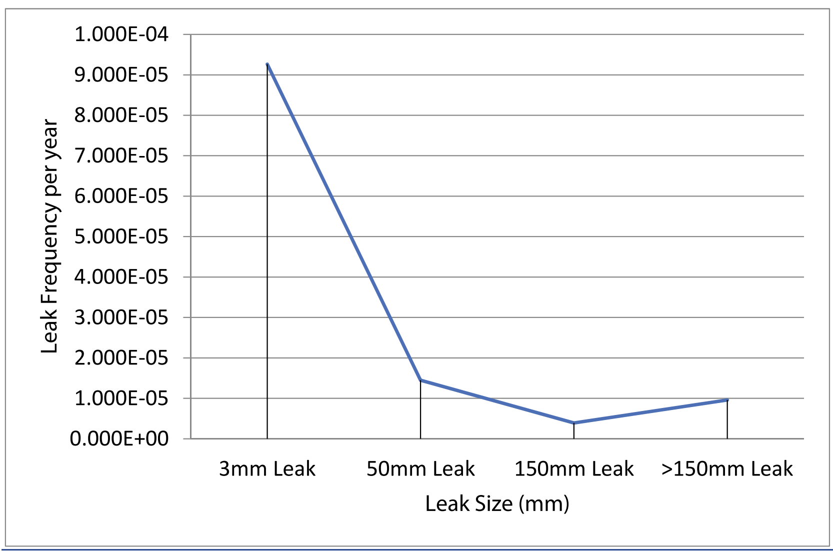

Figure 7. Leak frequency of designed bunkering system.

Table 3. Initial leak frequencies with respect to leak size.

		Frequency of Leak per year			
Equipment List	No. of Equipment	3mm Leak	50 m Leak	150 Leak	> 150 mm Leak
LNG Tank	1	9,459E-04	3,644E-04	1,350E-04	3,570E-04
Pressure Relief Valve	3	1,708E-03	1,778E-04	3,139E-05	5,945E-05
Pressure Indicator	2	6,214E-04	1,223E-04	5,047E-05	0,000E+00
Main Line Pipes	45	2,040E-03	2,997E-04	6,627E-05	2,966E-04
ESD Valves	4	2,277E-03	2,370E-04	4,186E-05	7,927E-05
Manual Valve	2	1,215E-04	2,514E-05	1,397E-05	0,000E+00
Main Line Flanges	12	7,383E-04	9,650E-05	1,873E-05	8,335E-05
Total Summation		8,452E-03	1,323E-03	3,577E-04	8,756E-04
Initial Frequency with Bunkering Duration		9,262E-05	1,450E-05	3,920E-06	9,596E-06

the bunkering process per year. Furthermore, the results of leakage frequencies show that the appearance of small holes is more common than that of larger size holes.

Safety measures and natural ventilation

IMO, through the International IGF Regulation, as well as other international bodies have established ventilation and safety measures for indoor areas, especially when it comes to transporting or processing dangerous goods indoors.

Through international IGF regulations, IMO and other international organizations have established ventilation and safety measures for indoor spaces, especially when transporting or handling dangerous goods indoors. As the bunkering process takes place in open spaces, ventilation is natural and there is no possibility of failure of mechanical ventilation systems, the requirements of international organizations do not apply. Furthermore, security and prevention automation measure due to the external installation of the system do not exist and the only way to prevent and timely action to limit any leakage is to have a watch-keeper. This case study assumes that in the event of a leak, the watch-keeper action is of high quality and a low risk of the leak. This leads to a limited leak with a 90% chance.

Probability of delayed ignition and immediate ignition

To calculate the probability of ignition, various models have been developed from time to time. The study adopted the Dutch model to calculate the immediate ignition (DNV 2012b). Table 4 shows the probabilities depending on the leak rate.

The Cox model was adopted in the calculation of the probabilities for delayed ignition, as it gives greater probabilities of ignition compared to other models. The following equation gives the Cox model (Cox, Lees, and Ang 1990). (Table 5)

$$PR_{DI} = 0.0158 * Q_{LR}^{0.6145} \qquad \text{Eq.(4)}$$

Due to the fact that both immediate ignition and delayed ignition probabilities are related to the leak rate and the equation of the initial leakage rate contains the density of the liquid, it was necessary to calculate the initial leak rate for LNG and LH_2 by the equation. 5 (DNV 2012a):

$$Q_L = C_D A \sqrt{2\rho_L[(P_O - P_a) + \rho_L g h]} \qquad \text{Eq.(5)}$$

Where:

Q_LInitial Liquid Rate (kg/s)
C_DDischarge Coefficient
AHole Area (m^2)
ρ_LLiquid Density (kg/m^3)
P_oInitial Pressure of Liquid (N/m^2)
P_αAtmospheric Pressure (10^5 N/m^2)
gGravity Acceleration (9.81 m/s^2)
hHeight of Liquid Surface above Hole (m)

Table 6 shows the results of the calculations for the initial liquid rate depending on the diameter of the holes.

Surrounding conditions

As a ship is a complex structure, the spaces are usually saturated. There are numerous systems such as piping, cranes, doors, etc. around the bunkering system. Thereby, it is assumed occupancy rate is of 20%.

Results of frequency evaluation

From the results collected in Table 7 for LNG and LH_2 respectively, it is clear that the ignition probability and result frequency are higher for LNG. More specifically, LNG has a greater ignition potential for pool fires in a hole with a diameter of 150 mm, in this case the difference between the two fuels is 5.00E-02.

Table 4. Immediate ignition probabilities.

Leak Rate (kg/s)	Immediate Ignition Probability
<10	0.02
10–100	0.04
>100	0.09

Table 5. Probability for delayed ignition with respect to initial liquid rate.

LNG PRDI	LH_2 PRDI
0.0031	0.0017
0.0986	0.0552
0.3803	0.2130

Table 6. Initial liquid release rate with respect to hole diameter.

Hole Diameter (mm)	LNG Initial Liquid Rate (kg/s)	LH_2 Initial Liquid Rate (kg/s)
3	0.071	0.028
50	19,674	7,662
150	177,065	68,959

The differences in the outcome frequencies of the two fuels are smaller, but LNG has an increased outcome frequency. The biggest difference between the two fuels is observed in a 150 mm diameter hole in the event of pool fire with the difference between the two fuels being of the order of 1.959E-07. Figure 8 illustrates the 9-point analysis of ignition probabilities and outcome frequencies for each fuel from Table 7 respectively. Points 1, 4 and 7 represent the ignition probabilities and outcome frequencies for pool fire, points 2, 5 and 8 for flash fire and 3, 6 and 9 for explosion for the two fuels respectively.

Consequence estimation

Table 7 shows the aggregated results of LNG & LH_2 consequence analysis. The initial leak frequency is indicated. After taking into account all factors that influence the bunkering process, the accompanying risks, and any combination of risks, the final estimate of the risk probability occurrence is indicated.

Table 7. Results of LNG & LH_2 consequence analysis.

	Hole Size	Initial Frequency	Fire Type	Immediate Ignition	Leak Duration	Ventilation System	Delayed Ignition	Surrounding Conditions	Ignition Probability	Outcome Frequency
LNG	3 mm	9.262E-05	Pool Fire	0.02	-	-	-	-	2.00E-02	1.852E-06
			Flash Fire	0.98	0.1	1	0.0031	0.8	2.43E-04	2.251E-8
			Explosion	0.98	0.1	1	0.0031	0.2	6.08E-05	5.628E-09
	50 mm	1.450E-05	Pool Fire	0.04	-	-	-	-	4.00E-02	5.798E-07
			Flash Fire	0.96	0.1	1	0.0986	0.8	7.57E-03	1.098E-07
			Explosion	0.96	0.1	1	0.0986	0.2	1.89E-03	2.744E-08
	150 mm	3.920E-06	Pool Fire	0.09	-	-	-	-	9.00E-02	3.528E-07
			Flash Fire	0.91	0.1	1	0.3803	0.8	2.77E-02	1.085E-07
			Explosion	0.91	0.1	1	0.3803	0.2	6.92E-03	2.713E-08
LH_2	3 mm	9.262E-05	Pool Fire	0.02	-	-	-	-	2.00E-02	1.852E-06
			Flash Fire	0.98	0.1	1	0.0017	0.8	1.33E-04	1.234E-08
			Explosion	0.98	0.1	1	0.0017	0.2	3.33E-05	3.086E-09
	50 mm	1.450E-05	Pool Fire	0.02	-	-	-	-	2.00E-02	2.899E-07
			Flash Fire	0.98	0.1	1	0.0552	0.8	4.33E-03	6.273E-08
			Explosion	0.98	0.1	1	0.0552	0.2	1.08E-03	1.568E-08
	150 mm	3.920E-06	Pool Fire	0.04	-	-	-	-	4.00E-02	1.568E-07
			Flash Fire	0.96	0.1	1	0.213	0.8	1.64E-02	6.412E-08
			Explosion	0.96	0.1	1	0.213	0.2	4.09E-03	1.603E-08

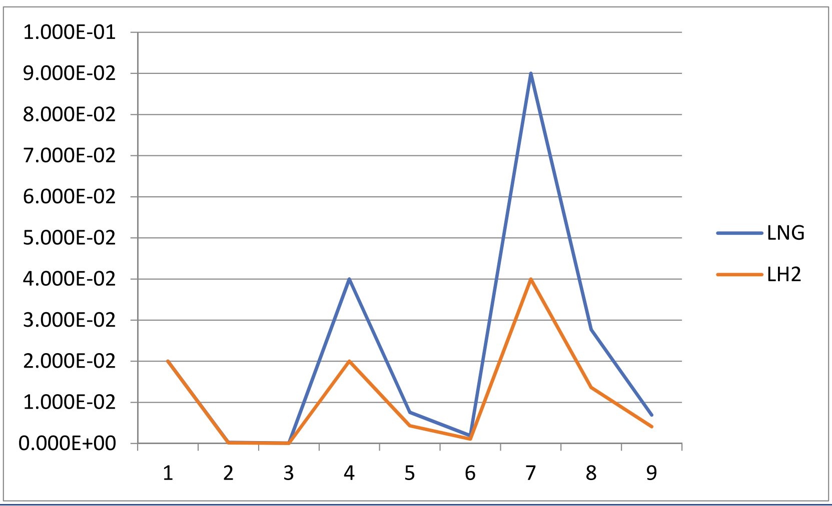

Figure 8. Comparison analysis of the ignition probabilities for LNG and LH_2 (a) & the outcome frequencies of LNG and LH_2 (b).

Vapour cloud explosion (VCE) model

A simplified TNT equivalent demonstration model analyzes the magnitude of the overpressure caused by the explosion of two fuels. This model was chosen for the simplicity and best assessment of damage over a specified distance (Rigas and Sklavounos 2002). The first step is to calculate the total leakage mass mT (kg) calculated from the product of the liquid velocity at the time of leakage according to the following equation:

$$m_T = Q_L * t_L \quad \text{Eq.(6)}$$

The leakage time in Eq. 6 is defined as the delayed isolation reaction of the watch keeper uses 30s to set the time limit for limited leaks (DNV 2012a).

The second step of the analysis is to calculate the total energy of the explosion that is converted into an equivalent mass of TNT by the equation:

$$W_{TNT} = \frac{m_v \eta \Delta H_{c(gas)}}{\Delta H_{c(TNT)}} \quad \text{Eq.(7)}$$

Where:

W_{TNT}Equivalent mass of TNT (kg)

m_vMass contributing to vapour cloud explosion (kg)

ηEmpirical explosion efficient (1% ~ 10%)

$\Delta H_{c(gas)}$Lower Heat of combustion of the material (kj/kg)

$\Delta H_{c(TNT)}$Heat of combustion of TNT (approximately 4,680 kj/kg)

The value of the empirical explosion efficient is traditionally set between 1% and 10%. For this study, the value of 10% is assumed in order to investigate the most difficult situation. The $\Delta H_{c(gas)}$ for LNG is assumed at 50,000 (kj/kg) and for LH_2 at 140,000 (kj/kg). Table 8 shows the total leak mass and energy converted into TNT equivalent mass for each of the two fuels with respect to the leaking holes.

Table 8. Leak mass & equivalent TNT mass for each fuel with respect to the size of the hole diameter.

Hole Diameter (mm)	LNG Total Leak Mass (kg)	LH_2 Total Leak Mass (kg)	LNG Equivalent TNT Mass (kg)	LH_2 Equivalent TNT Mass (kg)
3	0.708	0.276	0.756	0.825
50	196.738	76.621	210.190	229.208
150	1770.647	689.591	1891.716	2062.879

The next step is to determine the equivalent results for explosions that occur at a specified distance. This is expressed by Eq. 8. W_{TNT} is the equivalent mass calculated by Eq. 7 and for R_d, the values 50 m, 100 m, 500 m and 1,000 m are assumed.

$$Z_e = \frac{R_d}{(W_{TNT})^{1/3}} \quad \text{Eq.(8)}$$

Finally, the last step in determining overpressure is performed by Eq. 9:

$$P_s = 573 * Ze^{-1.685} \quad \text{Eq.(9)}$$

The calculations from the above equations are presented collectively for each fuel in Table 9 and Figure 9 for LNG and LH_2 respectively. From the results of Table 9 for LNG it is understood that the largest overpressure 54.437 kPa, appears at 150 mm diameter hole and for real distance at R_d 50 m, with scaled dimension at Z_e 4.043 m/kg$^{1/3}$. More specifically, Figure 9 (a) shows the results only for a 150 mm diameter hole, where the highest overpressure is observed.

Figure 9 (b) presents the results of the overpressure calculations for LH_2, where it is clear that the largest overpressure is found at the 150 mm diameter hole, for R_d 50 m and for scaled distance at Z_e 3.928 m/kg$^{1/3}$.

Comparing the final results of the two fuels which are LNG and LH_2, the highest overpressure for both fuels is found at the 150 mm diameter hole with an actual distance at Rd 50 m. The difference in overpressure between the two fuels is about 2.713 Pa. Therefore, it has been found that the overpressure of LH_2 can be more destructive than the overpressure of LNG. The calculations were made under the same conditions and on the same basis.

Lobato et al. (2009) show that installations with a wall thickness of 20–30 cm can be damaged in the case of an overpressure of 47–54 kPa.

Pool fire model

When two fuels are leaked during the bunkering process, the type of fire with the highest frequency of occurrence is pool fire. This study chose the model that has been selected to calculate the average length of the plume in relation to the diameter of the fire is

Table 9. LNG & LH_2 overpressure calculations.

LNG	R_d (m)	3 mm		50 mm		150 mm	
		Z_e (m/kg$^{1/3}$)	P_s (kPa)	Z_e (m/kg$^{1/3}$)	P_s (kPa)	Z_e (m/kg$^{1/3}$)	P_s (kPa)
	50	54.876	0.672	8.409	15.846	4.043	54.437
	100	109.752	0.209	16.819	4.928	8.086	16.930
	500	548.762	0.014	84.094	0.327	40.428	1.124
	1000	1097.524	0.004	168.188	0.102	80.856	0.350
LH_2	R_d (m)	3 mm		50 mm		150 mm	
		Z_e (m/kg$^{1/3}$)	P_s (kPa)	Z_e (m/kg$^{1/3}$)	P_s (kPa)	Z_e (m/kg$^{1/3}$)	P_s (kPa)
	50	53.308	0.706	8.170	16.636	3.928	57.150
	100	106.615	0.219	16.340	5.174	7.856	17.774
	500	533.077	0.015	81.701	0.344	39.278	1.180
	1000	1066.155	0.005	163.402	0.107	78.555	0.367

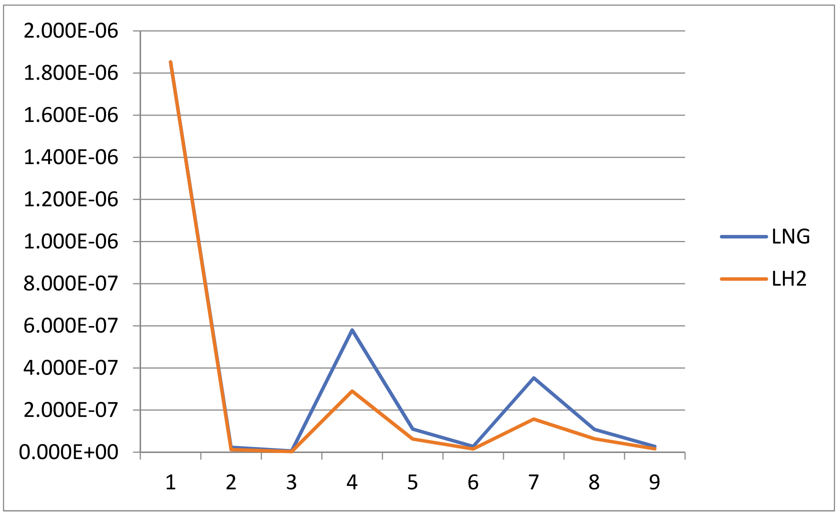

Figure 9. Overpressure vs. normalized distance for 150 mm diameter hole of LNG (a) & LH_2 (b).

derived and modified by Thomas (1965) to include the effect of wind on length.

The first step is to calculate the dimensionless wind speed using the following Eq.:

$$U^* = \frac{U_{wind}}{[(C_b/\rho_a)gD]^{1/3}} \qquad \text{Eq.(10)}$$

For this study, the following were assumed: neutral wind speed, U_{wind} = 5 m/s (DNV 2012b), density of air, ρ_{air} = 1.2 kg/m^3, and acceleration of gravity, g = 9.81 - m/s^2. As for liquid mass combustion flow, it was adopted at C_b = 0.14 kg/m^{2}s for LNG and for it was calculated at C_b = 0.31 kg/m^{2}s for LH_2 (Nedelka, Moorhouse, and Tucker 1989). The diameter D of the pool fire depends on the liquid leak rate (see Table 6) and the duration of the leak. In order to calculate the pool fire diameter in this study, the largest liquid rate was assumed, and as for duration of leakage, 10s was given to detect limited leaks. Another feature taken into account in the calculations of the diameter is the thickness of the pool, which is considered to be 100 mm for both fuels (DNV 2004). Table 10 clearly shows the calculated pool fire diameter, C_b that are used to calculate the dimensionless wind speed and the results of dimensionless wind speed using Eq. 10 for each fuel separately.

The next step is to calculate the Froude number through Eq. 11. All the coefficients of the Eq. are presented and analysed in the above paragraph. Table 10 shows the results of the calculations for each fuel separately.

$$F = \frac{C_b}{\rho_a * \sqrt{gD}} \qquad \text{Eq.(11)}$$

The next step is to calculate the plume length ratio in relation to the diameter of the fire using Thomas (1965) constraints and Eq. 12. The results of the Eq. are presented in detail in Table 10.

$$\frac{L_F}{D} = 55 * F^{\frac{2}{3}} * (U^*)^{-0.21} forF\langle 10^{-2} andU^* \rangle 1 \qquad \text{Eq.(12)}$$

From the above findings and analysis of the pool fire modeling results, the following conclusions are drawn. The number of Froude and the dimensionless wind speed U* depend on the diameter of the pool fire. Therefore, increasing the diameter reduces both the Froude number and U *. Secondly. the average value of the combustion flux, C_b, decreases significantly as the diameter of the pool fire increases due to heat absorption. The final results show that the height of the pool fire in the case of LH_2 is significantly bigger than of LNG. This difference in the values of the two fuels is also apparent in the ration of height to diameter; this is due to the fact that LH_2 is extremely buoyant.

Another issue with swimming pool fires is the radiation phenomena that occur during fires of both fuels. In order to proceed to a comparison of the radiation actions as well as the emission power resulting from the combustion of the two fuels, two leakage scenarios are compared for the maximum diameter hole that can occur in the bunkering system, that of 150 mm. As shown in Table 6, LNG leakage rate is 177.065 kg/s and for LH_2 is 68.959 kg/s. The energy produced due to the combustion of 1,770.65 kg LNG in 10s, using LHV, 50.02 MJ/kg, is 88,567.91 MJ. The corresponding energy for 689.59 kg LH_2, using LHV, 119.96 MJ/kg, is 82,719.62 MJ. From the above report, 10% of the LNG combustion energy

Table 10. Pool fire diameter and C_b for each fuel.

	LNG	LH_2
Liquid Leak Rate (kg/s)	177.065	68.959
Mean Value of Burning Flux, C_b (kg/m^{2}s)	0.140	0.270
Pool Fire Diameter, D (m)	7.330	11.135
Dimensionless wind speed, U*	2.461	1.720
Froude Number, F	1.376E-02	2.153E-02
Pool Fire Height to Diameter Ratio, L/D	2.614	3.798
Pool Fire Height, L	19.159	42.294

is converted into thermal radiation, where it translates to 8,856.79 MJ. On the other hand, the heat energy of hydrogen converted to thermal radiation is 4.5% which is 3,722.38 MJ. Thus, taking into account the diameter of the pool and the height of the flame from Table 10 and the thermal radiation analysed above for the two fuels, the fire emission power for LNG is 175.96 kW/m^2, whereas for LH_2 it is 97.57 kW/m^2.

As a result, hydrogen pool fire is of radiant nature, larger fire column and diameter compared to the corresponding elements of LNG, due to the fact that LH_2 is more intense as an element. On the other hand, hydrogen has lower thermal radiation than LNG and is strongly affected by atmospheric moisture.

Flash fire (Dispersion model) and impact

The risk level of flash fire is lower compared to pool or jet fire. the range of flash fire is estimated using the Gaussian model, which has the ability to predict downwind concentrations. The study use Brigg's coefficients (Briggs 1973). The general form of the Gauss model is expressed in Eq. 13 (Woodward and Pitbaldo 2010):

$$C(x,y,z) = \frac{F_{dis}}{2\pi u_w \sigma_y \sigma_z} exp\left[-\frac{1}{2}\left(\frac{y}{\sigma_y}\right)^2\right] \left\{ \exp\left[-\frac{1}{2}\left(\frac{z-H}{\sigma_z}\right)^2\right] + \exp\left[-\frac{1}{2}\left(\frac{z+H}{\sigma_z}\right)^2\right] \right\} \quad \text{Eq.}(13)$$

Since, leakage concentration is often expressed at ground level which means z = 0 and because H is in the same direction as z, therefore H = 0. Furthermore, due to the fact that the interest is focused on the highest concentration in the ground which is located along the centerline of the plume, then, y = 0 (Weiner and Matthews 2003). Therefore, because of the above explanations, Eq. 13 is converted to

$$C(x,0,0) = \frac{F_{dis}}{\pi u_w \sigma_y \sigma_z} \quad \text{Eq.}(14)$$

Where,

C(x,y,z)Concentration at some point in space (kg/m^3)

F_{dis}Release Rate (kg*s^{-1})

σ_y,σ_zConstants as functions of the downwind distance, x, (m)

u_{wind}Speed of Wind (m*s^{-1})

HHeight of the plume on centerline (m)

zDistance of crosswind (m)

yAbove the ground height (m)

From Eq. 14, it appears that the main aspect of the emission that need to be investigated are the release rate and the wind speed. The σ_y and σ_z are affected by wind speed as well as whether by it is day or night.

The analysis to find the concentration considers downwind distance, X, for 500 m, 100 m, 50 m and 10 m. Furthermore, day and night analysis are performed with a wind speed of 4.5 m/s which is an average wind value of Briggs data and σ_y and σ_z are calculated. F_{dis} is taken from Table 6 for the largest hole of 150 mm diameter for both fuels in order to calculate the most unfavorable leakage case.

Table 11 and Figure 10 show the results of the LNG and LH_2 concentration calculations, for daytime and night-time, at four selected distances in X-Direction.

As a result of calculating the concentrations of both fuels, it is clear that the highest concentrations are

Table 11. Concentration calculations of LNG and LH_2.

LNG		500 m	100 m	50 m	10 m
	Day	3.85E-03	9.08E-02	3.61E-01	8.96E+00
	Night	9.70E-03	1.93E-01	7.44E-01	1.80E+01
	Total (kg/m3)	1.35E-02	2.84E-01	1.10E+00	2.70E+01
LH_2		500 m	100 m	50 m	10 m
	Day	1.50E-03	3.54E-02	1.40E-01	3.49E+00
	Night	3.78E-03	7.51E-01	2.90E-01	7.02E+01
	Total (kg/m3)	5.28E-02	1.10E-01	4.30E+00	1.05E+01

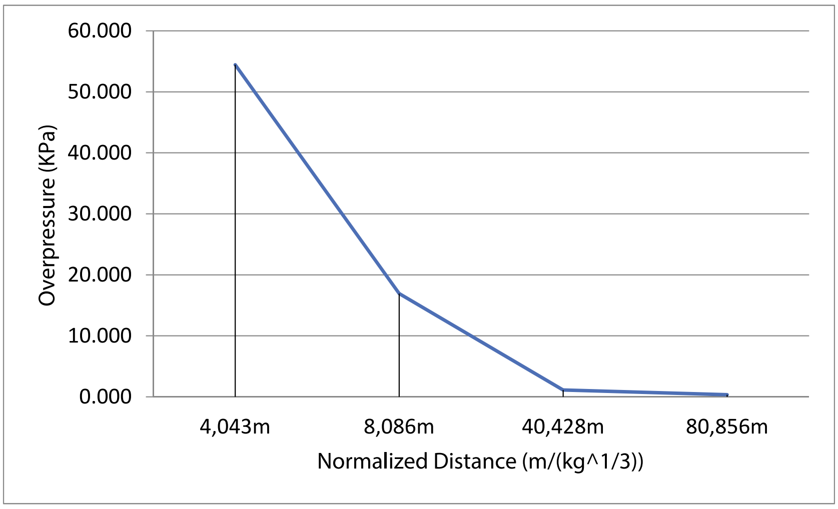

Figure 10. Concentration with respect to X-direction of LNG (a) & LH_2 (b).

observed in LNG at 10 m and 27 kg/m^3 in the X-direction compared to the highest concentration of LH_2 which is at 10 m and 10.51 kg/m^3 in the X-direction. In this particular case study, the rate of release of LNG is clearly higher than that of LH_2.

Establish safety exclusion zone

The determination of exclusion zones during the bunkering process of the two fuels is carried out by conducting a quantitative risk assessment not taking into account the factor of human presence such as the number of people involved in the bunkering process.

Fire and explosion are accompanied by a critical distance, which is directly related to the analysis of consequences as well as the probability of their occurrence. They cause heat transfer or overpressure. Thus, depending on their size, human injury can be provoked. The magnitude of thermal radiation and overpressure decreases as the distance from the flash point increases. Maximum radiation and overpressure prevail at the flash point. For the purposes of the current study critical thermal radiation is defined at 37.5 kW/m^2 and as critical overpressure at 1 bar for both LNG and LH_2 (Freeman 1990). In case of human exposure to the above values, there is certainty of death. LFL (5% for LNG and 4% for LH_2) will help research to extract critical distances for flash fire (Jeong et al. 2017).

Based on the above data and analysis of the consequences, Table 12 show the results with the critical distances for each consequence of each fuel.

Risk assessment

This study was conducted without considering the factor of human presence in the bunkering process. For this reason, the Dutch risk criterion with a frequency limit of 1.0E-6/year is used to define the exclusion zone (DNV 2012b).

Accidents can be classified into discrete zones based on the critical distances defined for each fuel in Table 12. The discrete zones for both fuels are shown in Table 13.

Specifically, the zone with a frequency higher than the acceptable limit (1.0E-6/year) can be considered an exclusion zone. Figure 11–15 and Table 14 show the risk level of discrete zones, as well as the exclusion zone for LNG and LH_2, which is Zone 3 (15–25 m) and Zone 2 (5–15 m) respectively. Also, the minimum distance for LNG and LH_2 in the exclusion zones is 5.9 m and 3.2 m respectively.

Discussion

The main goal of the project was to compare the two fuels LNG and LH_2 to reduce gaseous pollutants during bunkering of the bulk carrier chosen for this case study.

Table 12. Quantitative final results of LNG and LH_2.

	Hole Size	Initial Frequency	Fire Type	Immediate Ignition	Leak Duration	Ventilation System	Delayed Ignition	Surrounding Conditions	Ignition Probability	Outcome Frequency	Critical Distance (m)
LNG	3 mm	9.262E-05	Pool Fire	0.02	-	-	-	-	2.00E-02	1.852E-06	1.10
			Flash Fire	0.98	0.1	1	0.0031	0.8	2.43E-04	2.251E-8	4.50
			Explosion	0.98	0.1	1	0.0031	0.2	6.08E-05	5.628E-09	2.56
	50 mm	1.450E-05	Pool Fire	0.04	-	-	-	-	4.00E-02	5.798E-07	5.90
			Flash Fire	0.96	0.1	1	0.0986	0.8	7.57E-03	1.098E-07	75.00
			Explosion	0.96	0.1	1	0.0986	0.2	1.89E-03	2.744E-08	16.70
	150 mm	3.920E-06	Pool Fire	0.09	-	-	-	-	9.00E-02	3.528E-07	15.10
			Flash Fire	0.91	0.1	1	0.3803	0.8	2.77E-02	1.085E-07	203.00
			Explosion	0.91	0.1	1	0.3803	0.2	6.92E-03	2.713E-08	34.85
LH_2	3 mm	9.262E-05	Pool Fire	0.02	-	-	-	-	2.00E-02	1.852E-06	1.01
			Flash Fire	0.98	0.1	1	0.0017	0.8	1.33E-04	1.234E-08	3.20
			Explosion	0.98	0.1	1	0.0017	0.2	3.33E-05	3.086E-09	2.64
	50 mm	1.450E-05	Pool Fire	0.02	-	-	-	-	2.00E-02	2.899E-07	4.20
			Flash Fire	0.98	0.1	1	0.0552	0.8	4.33E-03	6.273E-08	55.00
			Explosion	0.98	0.1	1	0.0552	0.2	1.08E-03	1.568E-08	17.24
	150 mm	3.920E-06	Pool Fire	0.04	-	-	-	-	4.00E-02	1.568E-07	13.10
			Flash Fire	0.96	0.1	1	0.213	0.8	1.64E-02	6.412E-08	160.00
			Explosion	0.96	0.1	1	0.213	0.2	4.09E-03	1.603E-08	35.87

Table 13. Discrete zones with respect to the distance.

Discrete Zones	
Zone 1	Below 5 m
Zone 2	5–15 m
Zone 3	15–25 m
Zone 4	25–50 m
Zone 5	50–100 m
Zone 6	100–200 m
Zone 7	Over 200 m

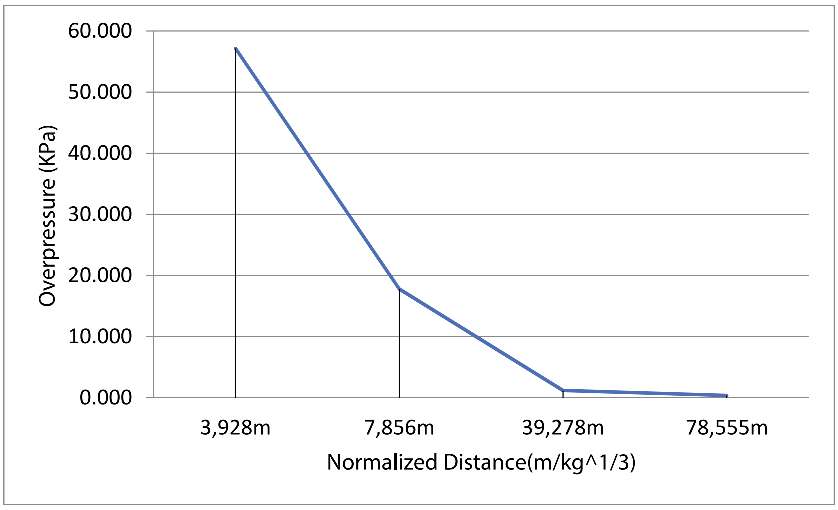

Figure 11. Safety exclusion zone and discrete zones of LNG (a) and LH_2 (b).

Table 14. Risk level of discrete zones of LNG and LH_2.

Radius (m)	0	5	15	25	50
LNG Risk Level per year	3.086E-06	1.205E-06	6.256E-07	2.454E-07	2.183E-07
LH_2 Risk Level per year	2.473E-06	3.153E-07	1.586E-07	1.429E-07	1.268E-07

The two fuels used in the study which are LNG and LH_2 were considered pure methane and pure hydrogen respectively.

In terms of bunkering system, this study leads to a proposal to redesign it, taking into account the LNG and LH_2 exclusion zones derived from the final results of the risk assessment. Another alternative can be to reinforce the safety system with double wall piping and an automatic leak detection system to minimize leaks and detection times. Furthermore, as one of the main factors that play an important role in determining the exclusion zone is the frequency of refueling, the longer the total time per year for refueling, the more exclusion zones should be expanded.

The study investigated the critical distances and the exclusion zones based on the limits of overpressure, pressure and radiation, which cause certain death. It should be noted that risks outside the defined exclusion zones may also occur with a lower probability of death, 70%, 50% and 10%.

The novelty of the current project lies in comparing two fuels that are trying to reduce gaseous pollutants in the field of safety during the bunkering process. This comparison, however, has the limitation of looking at only one aspect of the project.

This research was developed in a typical case study vessel during bunkering process. This in itself creates limitations for drawing more general conclusions. The bunkering process, based on the system design, takes

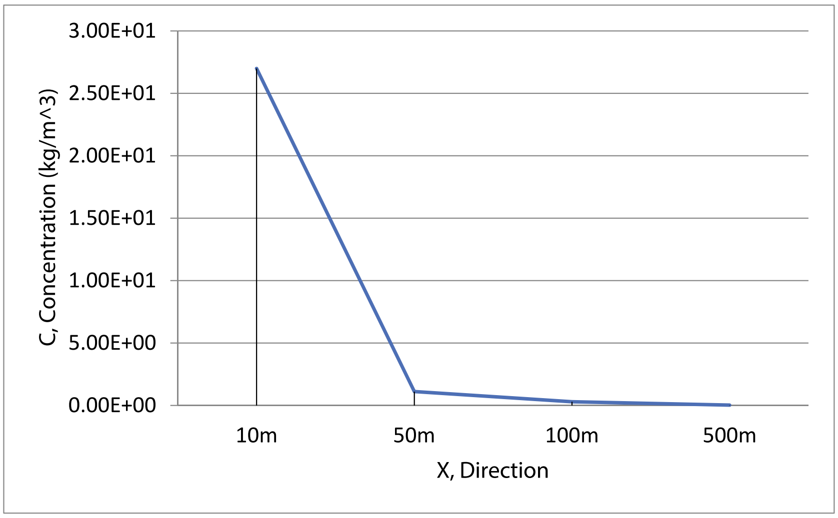

Figure 12. LNG Gas Concentration with respect to X-Direction

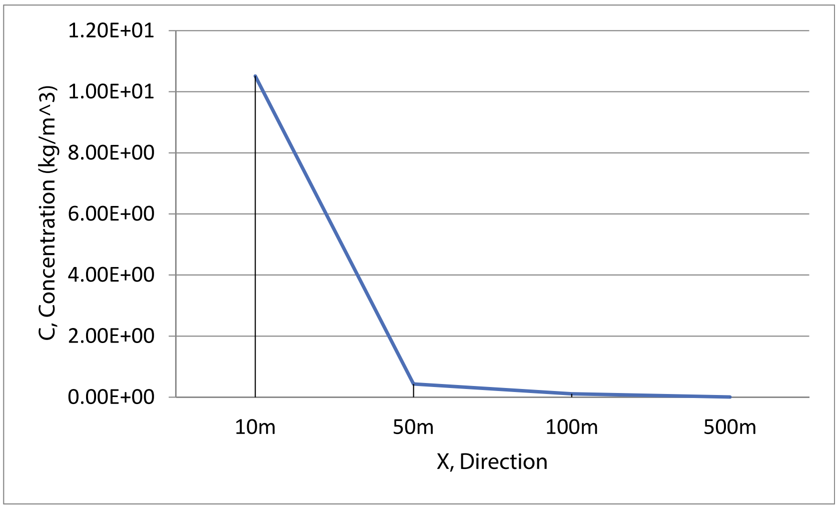

Figure 13. LH2 Gas Concentration with respect to X-Direction

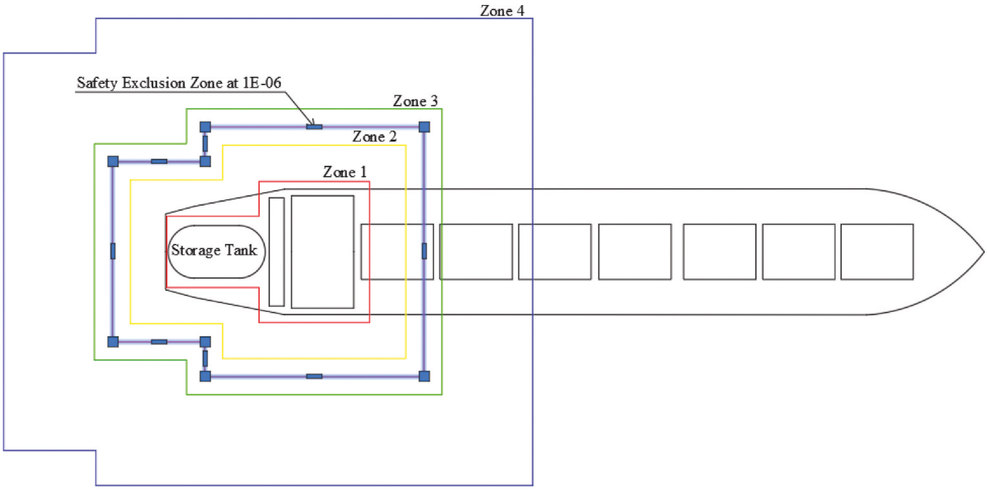

Figure 14. LNG Safety Exclusion Zone and Discrete Zones

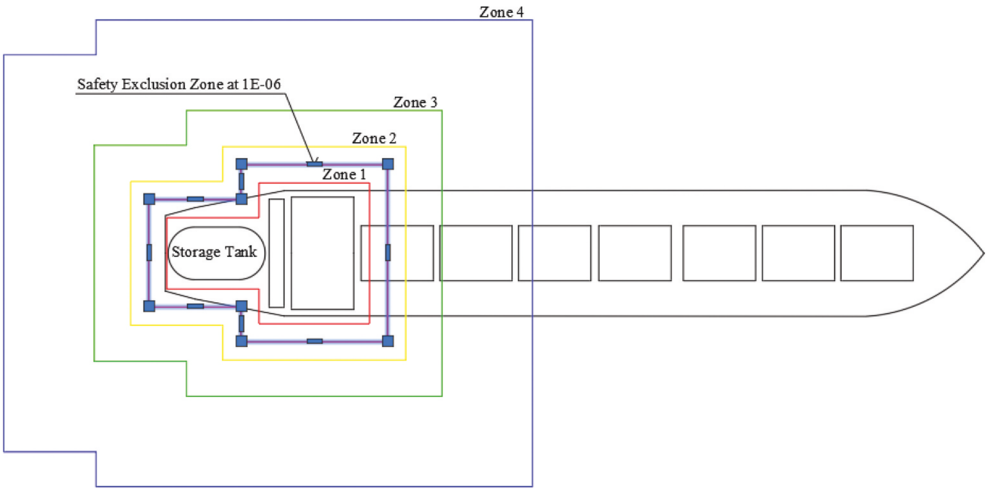

Figure 15. LH_2 Safety Exclusion Zone and Discrete Zones

place outdoors, so automatic leak detection systems are not taken into account in the study. The study did not estimate the financial losses that may be caused by the consequences of the leaks, nor did it take into consideration demographic conditions. Another limitation of the study mentioned in the previous paragraph of the chapter is that it dealt with leaks that may occur in components of the bunkering system and not from external factors.

In particular, since this study was developed on a typical case study vessel during the bunkering process, there are limitations in drawing general conclusions. It also does not take into account the automatic leak detection system, the financial losses and human factors that may cause as a result of the leak.

Thus, the next step of the study is to conduct experiments and studies in a wider range of applications. This will provide specific results on both fuels. The collection of data will lay the foundations for more thorough research in the future.

Conclusion

The study investigated and analysed the risks that may arise during the bunkering process of LNG and LH_2 using empirical models. Moreover, it evaluated and established exclusion zones for both fuels based on the Dutch risk criterion with frequency limit of 1.0E-6/year (DNV 2012b).

The most influential factor on the identification of exclusion zones as well as the level of risk of the bunkering process is the frequency of refueling and the time required to complete the process. The choice of larger piping for the system will increase the volume of fluid transfer and its speed, reducing the time required for the process. Reducing the required bunkering time also reduces ignition probabilities and outcome frequencies.

The LNG exclusion zone was observed to be one level bigger than LH_2. A comparison of the leakage of two fuels of the same energy showed that the leaks of LH_2 are smaller and have a shorter lifespan than those of LNG.

In the present study it was deemed appropriate not to use any software for the analysis of the case study, so that the frequencies and the consequence of the leaks could be developed more clearly. The analysis of the case study used certified data as well as empirical models to extract detailed results. It is advisable to use software in order to obtain more formal results.

Both fuels pose similar risks to the safety of the ship due to similar combustion and physical properties. It is advisable to take precautions to prevent fuel leakage, provide adequate ventilation in the room, minimize possible sources of ignition, and control fuel build-up at ignition limits.

In conclusion, this study sought to improve an overall understanding of the risks posed by the use and processing of LNG and LH_2 as fuel on merchant ships. There is an urgent need for a systematic study of the safety of LNG and LH_2 fuel lines, as well as the development of rules and regulations that provide clear guidance in accordance with the aforementioned studies.

Acknowledgments

The authors would like to express their gratitude to University of Strathclyde. This work is the product of the completion of a constructive and fruitful academic year at Strathclyde University, Department of Naval Architecture, Ocean and Marine Engineering (NAOME).

Disclosure statement

No potential conflict of interest was reported by the authors.

ORCID

Byongug Jeong http://orcid.org/0000-0002-8509-5824

References

ABS. (2014). "Bunkering of Liquefied Natural Gas-Fueled Marine Vessels in North America".

Aneziris, O., I. Papazoglou, M. Konstantinidou, and Z. Nivolianitou. 2014. "Integrated Risk Assessment for LNG Terminals." *Journal of Loss Prevention in the Process Industries* 28: 23–35. doi:10.1016/j.jlp.2013.07.014.

Briggs, G. 1973. "Diffusion Estimation for Small Emissions." In *Atmospheric Turbulence and Diffusion Laboratory Contribution. Technical Report 79*. Oak Ridge: National Oceanic and Atmospheric Administration.

Code, I. 2014. *International Code of Safety for Ship Using Gases or Other Low-Flashpoint Fuels*. London, UK: IMO.

Cox, A. W., F. P. Lees, and M. Ang. 1990. *Classification of Hazardous Locations*. Davis Building Railway Terrace Rugby CV21 3HQ, UK: IChemE.

DNV, G. (2004). LNG Marine Release Consequence Assessment.

DNV, G. 2012a. *Failure Frequency Guidance: Process Equipment Leak Frequency Data for Use in QRA*. Oslo: Det Norske Veritas (DNV).

DNV, G. (2012b). Port Toolkit Rist Profile LNG Bunkering.

DNV, G. (2014). Liquefied Natural Gas (LNG) Bunkering Study.

Farese, D., and S. Ivanova (2013). "Use Hydrogen Safely." www.aiche.org/CEP

Freeman, R. A. 1990. "CCPS Guidelines for Chemical Process Quantitative Risk Analysis." *Plant/Operations Progress* 9 (4): 231–235. doi:10.1002/prsb.720090409.

Jafari, M. J., E. Zarei, and N. Badri. 2012. "The Quantitative Risk Assessment of a Hydrogen Generation Unit." *International Journal of Hydrogen Energy* 37 (24): 19241–19249. doi:10.1016/j.ijhydene.2012.09.082.

Jeong, B., B. S. Lee, P. Zhou, and S.-M. Ha. 2017. "Evaluation of Safety Exclusion Zone for LNG Bunkering Station on LNG-Fuelled Ships." *Journal of Marine Engineering & Technology* 16 (3): 121–144. doi:10.1080/20464177.2017.1295786.

Klebanoff, L., J. Pratt, and C. LaFleur. 2017. "Comparison of the Safety-Related Physical and Combustion Properties of Liquid Hydrogen and Liquid Natural Gas in the Context of the SF-BREEZE High-Speed Fuel-Cell Ferry." *International Journal of Hydrogen Energy* 42 (1): 757–774. doi:10.1016/j.ijhydene.2016.11.024.

Lobato, J., J. Rodríguez, C. Jiménez, J. Llanos, A. Nieto-Márquez, and A. Inarejos. 2009. "Consequence Analysis of an Explosion by Simple Models: Texas Refinery Gasoline Explosion Case." *Afinidad* 66 (543): P372–379.

Nedelka, D., J. Moorhouse, and R. Tucker. 1989. *The Montoir 35m Diameter LNG Pool Fire Experiments*. London, UK: Midlands Research Station.

Qiao, A., and S. Zhang. 2010. "Advanced CFD Modeling on Vapor Dispersion and Vapor Cloud Explosion." *Journal of Loss Prevention in the Process Industries* 23 (6): 843–848. doi:10.1016/j.jlp.2010.06.006.

Rigas, F., and S. Sklavounos. 2002. "Risk and Consequence Analyses of Hazardous Chemicals in Marshalling Yards and Warehouses at Ikonio/Piraeus Harbour, Greece." *Journal of Loss Prevention in the Process Industries* 15 (6): 531–544. doi:10.1016/S0950-4230(02)00030-X.

Ruiz, P., L. F. Vega, M. D. M. Arxer, C. Jimenez, and A. Rausa. 2015. *Hydrogen: Applications and Safety Considerations*. Barchelona, Spain: MATGAS 2000 AIE.

Schlick, H. (2014). "Potentials and Challenges of Gas and Duel-Fuel Engines for Marine Application." Accessed June 25, 2020. https://www.cimac.com/cms/upload/events/cascades/cascades_2014_busan/presentations/Presentation_Session2_AVL_CASCADES_Busan_Oct2014_Harald_Schlick.pdf

Thomas, P. 1965. "Fire Spread in Wooden Cribs: Part III the Effect of Wind." *Fire Safety Science* 600: -1–1.

Weiner, R., and R. A. Matthews. 2003. *Chapter 18 - Meteorology and Air Pollution*. Burlington, MA: Elsevier Science.

Woodward, J. L., and R. Pitbaldo. 2010. *LNG Risk Based Safety: Modeling and Consequence Analysis*. NJ, USA: John Wiley & Sons.